

## Coupling shape-memory alloy and embedded informatics toward a metallic self-healing material

Lucia Faravelli\* and Alessandro Marzi

*Department of Structural Mechanics, University of Pavia, via Ferrata 1, Pavia, Italy*

*(Received December 7, 2009, Accepted June 3, 2010)*

**Abstract.** This paper investigates the possibility of a strategy for an automatic full recover of a structural component undergoing loading-unloading (fatigue) cycles: full recover means here that no replacement is required at the end of the mission. The goal is to obtain a material capable of self healing earlier before the damage becomes irreversible. Attention is focused on metallic materials, and in particular on shape memory alloys, for which the recovering policy just relies on thermal treatments. The results of several fatigue tests are first reported to acquire a deep understanding of the physical process. Then, for cycles of constant amplitude, the self-healing objective is achieved by mounting, on the structural component of interest, a suitable microcontroller. Its input, from suitable sensors, covers the current stress and strain in the alloy. The microcontroller elaborates from the input the value of a decisional parameter and activates the thermal process when a threshold is overcome.

**Keywords:** embedded informatics; fatigue tests; material recovery; self-healing; shape memory alloy.

---

### 1. Introduction

The European Science Foundation (ESF) and the US National Science Foundation (NSF) jointly sponsored a workshop, held in France in 2006, on Smart Structures (AFOSR/ARO/NSF/ONR/ESF 2006). The participants agreed on the need of a new vision for future structures. They will be capable of self-sensing and monitoring, self-diagnosis and prognosis with intelligence, self-healing and repair, as well as adaptive response to prevent loss of human life and catastrophe, to minimize maintenance and life-cycle costs and to prolong service life.

Such structures will be made of multi-functional materials integrated with sensors, actuators, electronics and intelligence software to perform a variety of functions. With smart sensing and intelligent diagnostics, the structural condition will be monitored and the residual life will be predicted while the structures are in service. Optimal structural performance will be achieved in operation because the actual structural conditions will be better known in real time and because the structures will be more adaptive to changes. Embedded sensory network and nervous system are envisaged to have self-communication with maintenance crew. Operation and maintenance cost are minimized in this way, while the economic life of structures is extended.

Within this smart system technology, two terms were introduced to cover the dream of obtaining fully self-sufficient (bio-inspired) systems: “autonomics” covers systems with sensors, informatics and

---

\*Corresponding Author, Professor, E-mail: [lucia@dipmec.unipv.it](mailto:lucia@dipmec.unipv.it)

actuators able to counteract likely aggressions from the external environment; “self-healing materials” covers those (composite) materials showing sensitive features and capability of repairing damage, when detected (Van der Zwaag 2007).

This paper focuses on the second concept. Its original target only demands that the repaired region across the material shows a residual lifetime allowing the structural system to complete the mission. After that, the damaged structural component must be replaced.

This paper considers metallic materials and in particular an alloy of the class of the shape memory alloys (SMA) (Auricchio *et al.* 2001). The possibility of a strategy for an automatic full recover of the material after it underwent several fatigue cycles is investigated experimentally and the results are discussed.

This paper experimentally investigates the effect of heat treatment on the recovery of the functionality of SMA bars under fatigue loading. Since details on the specific tested alloy, and on the way its specimens were tested, are provided in reference (Casciati and Van der Eijk 2008), the reader is referred to such a paper for a deep description of the raw materials (composition, maximum strain, strength, modulus, etc.), specimen preparation (dimension, number of specimens, etc.), experiment (machine used, standard followed, loading details, etc.), instrumentation (strain measurement, stress measurement, etc.). In this manuscript only the items necessary for a self-consistent assemblage process of the results are reported.

Furthermore, a reader looking for a motivation for the consideration of the specific problem is referred to references (Casciati and Hamdaoui 2008, Chrysostomou *et al.* 2008) reporting the results of the EU funded project WINDCHIME, suggesting the adoption of pre-tensioned SMA bars for the retrofit of the monumental cultural heritage.

## 2. The self-healing concept and SMA

The fascinating concept of self-healing material covers at the moment three main classes of technological realizations:

- materials which incorporate a sensing-counteracting automatic trick (AFOSR/ARO/NSF/ONR/ESF 2006, Van der Zwaag 2007). They must be regarded as two stages materials: the initial state is replaced by an updated configuration after the recovering caused by a undesired event;
- materials which mount a sensing-counteracting loop driven by a micro-controller (Casciati and Rossi 2006), i.e., where the self-healing concept assumes an informatics meaning;
- materials which utilize special mechanical features to recover their initial state even after hysteretic cycles (Auricchio *et al.* 2001).

The super-elastic property ensuring the third kind of behaviour is a special feature of shape memory alloys. Shape memory alloys in the austenite state show particular properties associated with their martensitic transformation between metastable phases. The pseudo-elasticity and thermo-elasticity are effects related to their phase transition and used in sensors and actuators. The transformation, often referred to as a first order phase transition with latent heat, shows hysteresis. The hysteretic behavior in this solid-solid transformation can be used in structural subcomponents to mitigate the unwished vibration effects of external dynamic actions (Casciati and Faravelli 2009). The goal can be pursued either by dissipating energy in hysteretic cycles or allowing significant deformations without stress losses. Since the deformations are fully recovered when the dynamic actions stop, the re-centring property comes implicitly with the adoption of such alloys.

The more commonly adopted materials are Ni-Ti alloys (Casciati and Van der Eijk 2008), for structural elements of small size (say 1 mm or less of thickness), and Cu-based alloys when component of larger size must be built. Attention is focused in this contribution on an alloy mixing Cu, Al and Be (Casciati and Van der Eijk 2008, Casciati and Faravelli 2008).

The alloy is cast in ingots which are then transformed into suitable structural elements as wires, bars or plates. A mechanical testing, at this stage of the production, shows a super-elastic hysteretic diagram which deteriorates as loading-unloading cycles are repeated. Actually, there is a trend to produce martensite during each cycle and this results in residual deformations.

The inconvenience is reduced by a suitable initial thermal treatment. It reduces drastically the level at which the strain increases without significant variations of the stress, but stabilizes the cycles more and more depending on the treatment duration. As a result, the designer must afford an optimization problem accounting for the marginal hysteretic amelioration versus the material weakening (Casciati 2007).

This paper studies the possibility of merging the second and the third of the three classes listed at the beginning of this section toward the realization of a self-recovering material, i.e., the idea of adding informatics to SMA components realize a self-healing solution is investigated.

### 2.1 Fatigue response

The first idea of testing the alloy under repeated loading-unloading cycles in view of assessing its fatigue performance dates back 20 years (Van Humbeeck 1991). Nevertheless, most of the existing literature is focused on the response of Ni-Ti alloys (Tabanlı *et al.* 1999, Shimamoto *et al.* 2004, Dolce and Cardone 2005, Nayan *et al.* 2008) apart for the results reported in (Casciati *et al.* 2008) and related studies (Casciati *et al.* 2007, Casciati and Faravelli 2006), which also cover the Cu-based alloy considered in this paper. The studies on the Cu-based alloy can be synthesized as follows.

The axial test of a SMA specimen under loading-unloading, in controlled thermal environment, can be expressed for the single cycle by the relationship

$$\sigma(t) = \sigma(\varepsilon(t), \varepsilon_{\max}, \varepsilon_{\min}, \sigma_{\max}, \sigma_{\min}, \eta | \Theta, \Gamma, f_c) \quad (1)$$

where  $\sigma(t)$  is the stress at time  $t$ ;

$\varepsilon(t)$  is the strain at time  $t$ ;

$\varepsilon_{\max}, \varepsilon_{\min}$  are the upper and lower limit of the strain during the cycle, respectively;

$\sigma_{\max}, \sigma_{\min}$  are the upper and lower limit of the stress during the cycle, respectively;

$\eta$  is a dimensionless hysteresis loop dimension;

$\Theta$  is the temperature of the controlled environment;

$\Gamma$  is a parameter marking the specific thermal treatment of the specimen;

$f_c$  is the frequency of the cycles.

The definition of  $\eta$  requires the introduction of the energy dissipated per cycle, computed as

$$\mathfrak{I}_c = \oint P du = \oint \sigma A d\varepsilon L_0 = V_0 \oint \sigma d\varepsilon \quad (2)$$

where  $A$  and  $L_0$  denote the cross section area and the initial length, respectively, of the specimen,  $P$  the tension load and  $u$  the specimen elongation which coincides with the test machine span. If a single cycle is approximated by an ellipse of diameters  $d$  and  $\eta d$ , with  $d$  given by

$$d = \sqrt{(\sigma_{\max} - \sigma_{\min})^2 + (\varepsilon_{\max} - \varepsilon_{\min})^2} \quad (3)$$

The energy per cycle can then be written

$$\mathfrak{S}_c = \pi \eta d^2 / 4 \quad (4)$$

and this equation is used to assess the value of  $\eta$ . During a fatigue test, the subsequent values assumed by this parameter denotes the degradation of the loop, which is associated with the changes in phase of the alloy components. This change in phase is also made evident by the degradation of the stress levels. Such a remark suggests to avoid performing fatigue tests in load control between stress lower and upper limits. By contrast, two policies can be envisaged:

a) span control between lower and upper limit of the strain, denoted as type A in the following

$$\sigma(t) = \sigma(\varepsilon(t), \sigma_{\max}, \sigma_{\min}, \eta | \Theta, \Gamma, f_c, \varepsilon_{\max}, \varepsilon_{\min}) \quad (5)$$

b) span control from zero load to the maximum strain and load control for the unloading to zero load (say type B):

$$\sigma(t) = \sigma(\varepsilon(t), \varepsilon_{\min}, \sigma_{\max}, \eta | \Theta, \Gamma, f_c, \varepsilon_{\max}, \sigma_{\min}) \quad (6)$$

The consequences of these two approaches will be discussed later. It is just worth noticing that the phase-change/degradation is monitored by the stress and/or strain limits which are not assigned for that particular cycle.

For sake of clarification, “span” is referred to the kinematics of the upper grip of the universal testing machine and is measured by an incorporated LVDT (Linear Variable Differential Transducer). It is “de facto” the elongation of the tested bar: divided by the initial length of the bar one finds an average deformation. By contrast, if an extensometer is mounted, the test can be driven by the read strain and one would speak of test carried in “strain control”. The other physical parameter is the applied load, read by an incorporated load cell. The stress is simply obtained by dividing the load by the initial area of the bar cross-section.

A further remark is preliminarily required. The use of SMA structural elements requires a deep knowledge of SMA properties and their coherence with the application requirements. For instance, in earthquakes engineering, after several years or decades at rest, the material is required to undergo some as 200 oscillations when the shock occurs (Casciati *et al.* 2008). The mechanical analysis of the energetic conversion, from mechanical energy to heat, suggests the advantages of pre-stressed SMA (Casciati and Hamdaoui 2008). But, using Cu-based alloys pre-stressing can modify the thermo-mechanical behavior of the alloy via the martensite stabilization and this means that suitable periodic maintenance is required. In general diffusion effects should be carefully studied and quantified for any long duration application (Terriault *et al.* 2007, Torra *et al.* 2007).

## 2.2 Annealing

“Shape memory alloys (SMA) suffer from the same impairing mechanisms experienced during cycling loading by classic alloys. Moreover, SMA fatigue behaviour is greatly influenced by thermo-mechanical cycling through the zone of thermo-elastic phase transformation, which is the basis of shape memory and super-elasticity effects” (Brailovski *et al.* 2002). The fatigue resistance of any material can be improved by an appropriate thermo-mechanical treatment. The annealing heat treatment,

whose parameters are temperature and duration, is generally intended to regulate shape memory properties of the cold-worked material and to set a shape into the material. An optimum trade-off in two properties should guarantee the best dimensional and functional stability of SMA devices: the mechanical work which could be generated by SMAs upon heating and the true yield stress.

The approach of using annealing for “healing” a “fatigued” metal is not new (Ding *et al.* 2007), even if, once again, most of the literature is simply focused on Ni-Ti alloys. In addition, this paper is mainly focused on what parameters could provide a feedback in a control system.

### **3. Preliminary fatigue tests**

The Cu-based alloy which was selected among those available on the market has per cent weights of 11.8 for Al and 0.5 for Be. It is cast in ingots of 6 kilos, from which specimens in form of bars were obtained. The following phase transformation temperatures were obtained by the Differential Scanning Calorimeter (DSC) test on the material as produced: martensite starts at -46 °C; martensite finishes at -55 °C; austenite starts at -25 °C and austenite finishes at -18 °C. Details on the material and on the tests conducted on it can be found in (Casciati and Van der Eijk 2008) and (Casciati *et al.* 2007, Casciati and Faravelli 2006), respectively. Reference (Casciati *et al.* 2007) reports the results of fatigue tests in tension, while reference (Casciati and Faravelli 2006) reports fatigue tests in torsion.

This first test campaign was carried out in span (i.e., displacement) control (type A test) between assigned lower and upper bounds. The specimens were selected to have a pipe section so that possible undesired compression states do not affect significantly the test. The specimens were obtained from bars of external diameter 15 mm, removing the internal material to form a pipe of internal diameter either 12 mm or 12.5 mm.

The single specimen should undergo a thermal treatment before the test to improve the alloy response in the range of strain up to the 4%. The treatment consists of 4 minutes at 850°C, then out at ambient temperature (water quenched), and finally 2 hours at 100°C. Tests after such a treatment emphasize that:

- i. the plateau level, in the stress-strain plot, is significantly decreased by the thermal treatment;
- ii. in tension there is a good recover of strain, after unloading, even after a loading up to 6% of deformation;
- iii. in compression, un-recovered strains are recorded, after unloading, for any level of peak deformation.

The following remarks summarize the main feature of the laboratory experience:

- a) The material virgin curve is abandoned after the first unloading. The higher is the strain reached during the loading, the wider is the gap, which stabilizes after some cycles of the same amplitude;
- b) The first unloading produces small residual strains, which are due to some martensite volume which does not recover into austenite; the residual strain becomes significant when a strain of 5-6% is reached during the loading cycle;
- c) Unloading is badly conducted in displacement control; indeed, at very low values of strain, the residual displacements are associated with compression loads;
- d) Unloading can be correctly performed in force control, but the machine allows it only for specimens of significant section. In other words it does not apply to wires. It will be adopted in the subsequent tests (Section 4) conducted on bars of circular solid section.

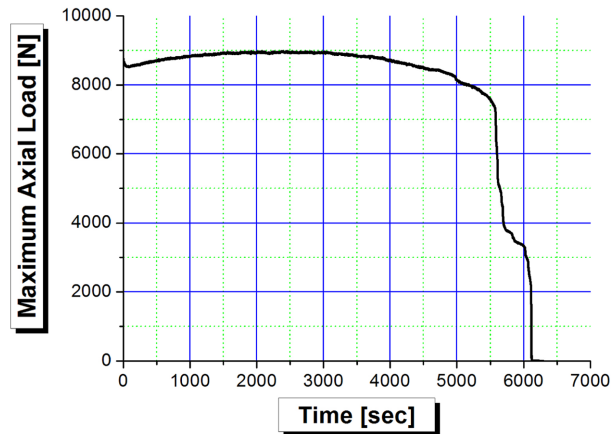


Fig. 1 Time history of the maximum axial load recorded during a series of loading-unloading cycles in tension at frequency  $f_c = 1$  Hz and temperature  $\Theta = 30$  °C;  $\varepsilon_{\max} = 2\%$ ,  $\varepsilon_{\min} = 0.5\%$

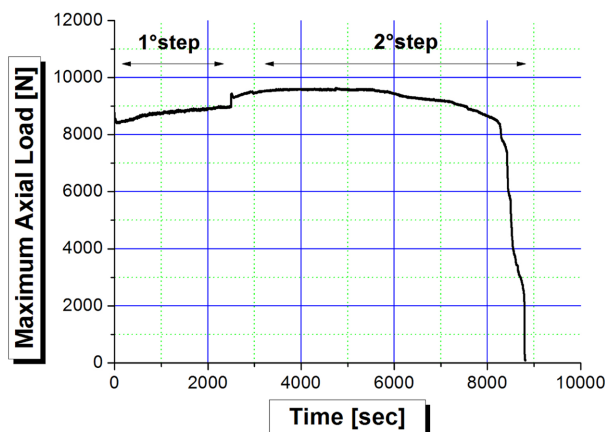


Fig. 2 Time history of the maximum axial load recorded during a series of loading-unloading cycles in tension at frequency  $f_c = 1$  Hz and temperature  $\Theta = 30$  °C;  $\varepsilon_{\max} = 2\%$ ,  $\varepsilon_{\min} = 0.5\%$ . The test is the same as in Fig. 1, but after 2500 cycles it was interrupted and the specimen heated at 280 °C for half hour

Fig. 1 is an example of the results achieved in this preliminary campaign of tests. The specimen with pipe cross-section is tested in the range of strain ( $\varepsilon_{\min}$ ,  $\varepsilon_{\max}$ ) from 0.5% to 2%. The test is carried out at the frequency rate  $f_c = 1$  Hz and at the temperature of  $\Theta = 30$  °C. As reported in (Casciati 2007), the test was repeated and stopped after 2500 cycles in order to heat the specimen at 280 °C for half hour. The test was then restarted and the specimen can perform after the interruption a number of cycles to rupture equal to the one achievable on a new specimen (Fig. 2). In other words, the specimen performed as all the first set of cycles was not “remembered” by the alloy. In Fig. 2, as well as in the following graphs associated with tests with annealing interruptions, the resting period was not reported in the figures.

To make this a self healing scheme, some informatics must be added (Casciati 2007): it was suggested that it should count the loading-unloading cycles and automatically start the heating

process at one half or less of the expected lifetime.

All the tests discussed in this and next sessions of the paper are synthesized in Table 1 to improve the readability and to facilitate the comparisons.

#### 4. Fatigue tests in span control

Reference (Casciati *et al.* 2008) is motivated by the wish of having several laboratories all around the world producing tests whose results can be compared and assembled. Therefore, a common specimen was introduced. It was obtained by bars of diameter 3.5 mm and each test is conducted at the frequency of one cycle per second with the main variables recorded 16 times per second. The preliminary thermal treatment consists of 5 minutes at 850 °C, then out at ambient temperature (water quenched), and finally 2 hours at 100 °C.

Of course the main output is given by the triplet: upper strain, strain range, number of cycles to failure, the values being reported in Table 2 for the tests summarized in Table 1. With a higher number

Table 1 Summary of the parameters which characterize the fatigue tests discussed along the paper

| Test number<br>& control type | Figure<br>number | $\varepsilon_{\min}$<br>% | $\varepsilon_{\max}$<br>% | $\sigma_{\min}$<br>[MPa] | $\sigma_{\max}$<br>[MPa] | $f_c$<br>[Hz] | $\Theta$<br>[°C] | $\Gamma$                       | Healing   |
|-------------------------------|------------------|---------------------------|---------------------------|--------------------------|--------------------------|---------------|------------------|--------------------------------|-----------|
| 1 - A                         | 1                | 0.5                       | 2                         | 41<br>-14                | 141.2<br>114             | 1             | 30               | 4 min 850 °C + 2h 100 °C       | /         |
| 2 - A                         | 2                | 0.5                       | 2                         | 73<br>15                 | 151.5<br>125.8           | 1             | 30               | 4 min 850 °C + 2h 100 °C       | 1/2h 280° |
| 3 - A                         | 3 & 4            | 3.6                       | 5.2                       | 180<br>52.8              | 280.5<br>199.1           | 1             | 30               | 5 min 850 °C + 2h 100 °C       | /         |
| 4 - A                         | --               | 1.2                       | 4.3                       | 81.4<br>-27.7            | 243.9<br>165.9           | 1             | 30               | 5 min 850 °C + 2h 100 °C       | /         |
| 5 - A                         | 5/6              | 1.2                       | 4.3                       | 70.3<br>-22.3            | 204.5<br>143.2           | 1             | 30               | 5 min 850 °C + 2h 100 °C       | 2h 100 °C |
| 6 - A                         | --               | 1.2                       | 4.3                       | 124.2<br>-10.9           | 262.4<br>209.8           | 1             | 50               | 5 min 850 °C + 2h 100 °C       | /         |
| 7 - A                         | 7                | 1.2                       | 4.3                       | 129.419                  | 226.8<br>154.9           | 1             | 50               | 5 min 850 °C + 2h 100 °C       | 1/2h 280° |
| 8 - B                         | Casciati**       | 0.5<br>0.9                | 3.2                       | 0                        | 227.5<br>200             | 0.5           | 30               | 10 min 850 °C + 1week 100 °C * | /         |
| 9 - B                         | 8                | 0.3<br>1.2                | 3.2                       | 0                        | 200.9<br>127.8           | 0.5           | 30               | 10 min 850 °C + 2h 100 °C      | 1/2h 280° |
| 10 - B                        | 9                | 0.33<br>1.3               | 3.2                       | 0                        | 208.5<br>105.3           | 0.5           | 30               | 10 min 850 °C + 1week 100 °C   | 1/2h 280° |
| 11 -B                         |                  | 0.4<br>1.09               | 3.0                       | 0                        | 200<br>115               | 0.5           | 50               | 10 min 850 °C + 2h 100 °C      | /         |
| 12 - B                        | 10               | 0.4<br>1.0                | 3.0                       | 0                        | 187<br>150               | 0.5           | 50               | 10 min 850 °C + 2h 100 °C      | 1/2h 280° |

\*plus a preliminary mechanical training consisting of series of 50 cycles ( $f_c = 0.25$  Hz), each up different upper value of the strain (up to 0.8%, 1.2%, 1.5%, 2.3% and 3.2%) of at the temperature of 34 °C

\*\*Casciati *et al.* (2008)

Table 2 Main results from the fatigue tests of Table 1

| Test number & control type | Figure number | $\varepsilon_{\max}$ % | $\varepsilon_{\max} - \varepsilon_{\min}$ % | Cycles step 1 | Cycles step 2 | Cycles step 3 | Healing   |
|----------------------------|---------------|------------------------|---|---------------|---------------|---------------|-----------|
| 1 - A                      | 1             | 2.0                    | 1.5   | 6297          | --            | --            | /         |
| 2 - A                      | 2             | 2.0                    | 1.5   | 2500          | 6397          | --            | 1/2h 280° |
| 3 - A                      | 3 & 4         | 5.2                    | 1.6   | 15047         | --            | --            | /         |
| 4 - A                      | --            | 4.3                    | 3.1   | 2037          | --            | --            | /         |
| 5 - A                      | 5/6           | 4.3                    | 3.1   | 1028          | 1028          | 2262          | 2h 100 °C |
| 6 - A                      | --            | 4.3                    | 3.1   | 1800          | --            | --            | /         |
| 7 - A                      | 7             | 4.3                    | 3.1   | 800           | 800           | 2261          | 1/2h 280° |
| 8 - B                      | Casciati*     | 3.2                    | varying                                     | 2120          | --            | --            | /         |
| 9 - B                      | 8             | 3.2                    | varying                                     | 1002          | 1002          | 5701          | 1/2h 280° |
| 10 - B                     | 9             | 3.2                    | varying                                     | 1002          | 1002          | --            | 1/2h 280° |
| 11 - B                     | --            | 3.0                    | varying                                     | 3939          | --            | --            | /         |
| 12 - B                     | 10            | 3.0                    | varying                                     | 1703          | 1703          | 13734         | 1/2h 280° |

\*Casciati *et al.* (2008)

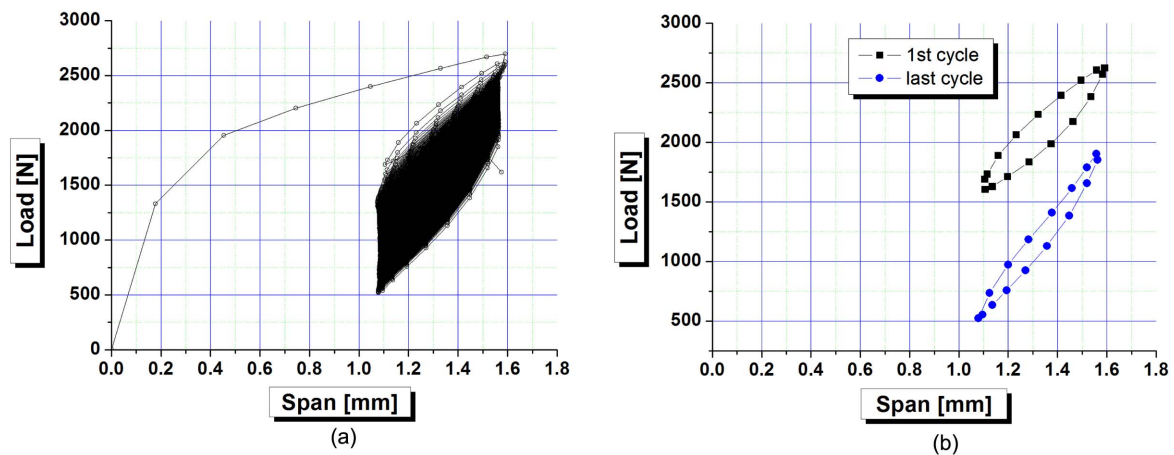


Fig. 3 Fatigue test between 3.6% and 5.2% of strain at 30 °C: (a) the whole load-span time history and (b) first unloading-loading cycle and cycle 15108 (the last one)

of sampling points per cycles, several options can be considered in terms of graphical representation.

In Fig. 3(a), one sees the whole time history as recorded in term of load vs. span (i.e., equivalently, stress vs. strain). For this special case, where the deformation ranges between 3.6% and 5.2% and the temperature is 30 °C, the repeated loading-unloading cycles have the effect of producing a loop with these characteristics: the maximum load has a value lower and lower and the loop shape is thinner and thinner as the test proceeds. This is why Fig. 3(b) only provides the first unloading-loading cycle and the last one: in this way the loop deterioration is better appreciated.

Alternatively, one computes the dissipated energy per cycle (from Eq. (2)) and plots it vs. the number of cycles. In this way the graph of Fig. 4(a) is obtained, where a nearly linear trend characterizes the central part of the curve. The loop deterioration at the beginning of the test is a

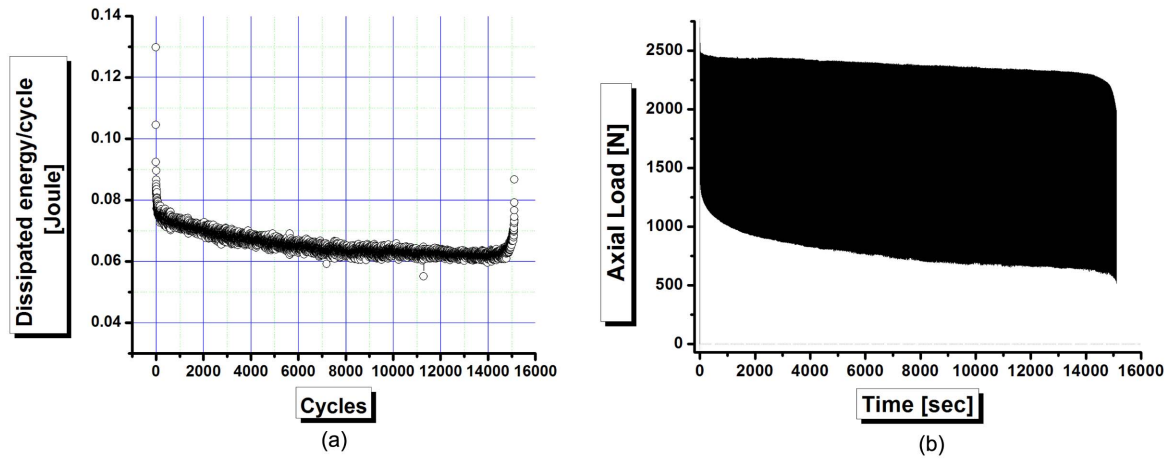


Fig. 4 Fatigue test between 3.6 and 5.2% of strain at 30 °C: (a) the trend of dissipated energy per cycle and (b) maximum-minimum load cycles

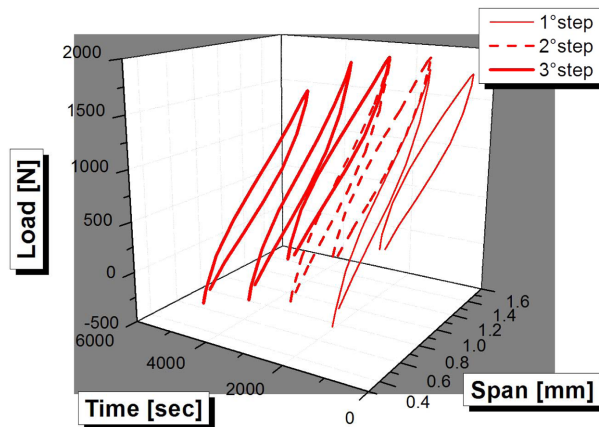


Fig. 5 Fatigue test between 1.2% and 4.3% of strain at 30 °C: first part of the test up to 1028 cycles; second part of the test with further 1028 cycles; third part of the test with further 2262 cycles

well-known feature of these alloys. The increasing tail is related to the displacement control adopted during the test: indeed, the minimum strain after unloading is reached, in the last cycles, at lower and lower values of the load, thus enlarging the loop. Furthermore, a typical representation of the results (maximum-minimum loads vs. number of cycles) is given in Fig. 4(b), where, once again, one detects the two aspects of the deterioration: the maximum load decreases as the test proceeds, while the minimum load decreases even faster, giving rise to the counter-clockwise rotation of the loops emphasized in Fig. 3(b).

Several tests similar to the one summarized in Figs. 3 and 4 were carried out. One of them is synthesized as test 4 in Tables 1 and 2 and was run at  $\theta = 30\text{ }^{\circ}\text{C}$ . The one marked as test 6 was run at  $\theta = 50\text{ }^{\circ}\text{C}$ .

With reference to test 4 in Table 1, the test is repeated (test 5) by interrupting it after 1000 cycles. The thermal treatment which complete the initial preparation (2 hours at 100 °C) is repeated. The test re-starts and stops again after further 1000 cycles and new thermal treatment. Eventually, third

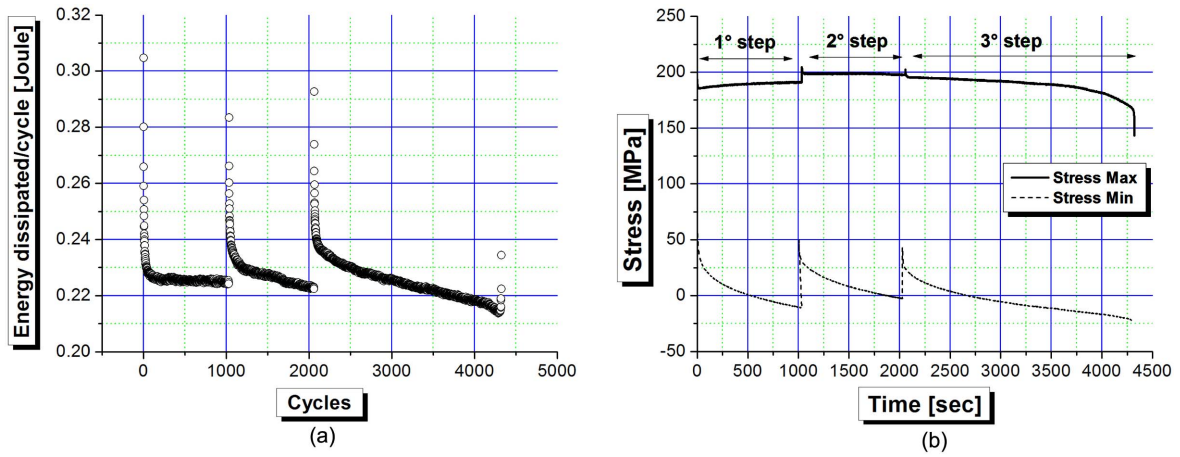


Fig. 6 Fatigue test between 1.2% and 4.3% of strain at 30 °C: first part of the test up to 1028 cycles; second part of the test with further 1028 cycles; third part of the test with further 2262 cycles. (a) energy dissipated per cycle and (b) maximum and minimum stresses as the cycles proceed

stage of the test up to final rupture. The second and final cycles of the three 1000 cycles sequences are drawn in Fig. 5 together with the last cycle before failure (Faravelli 2008).

Moving to the representation adopted in Fig. 4, one obtains the plots of Fig. 6, where Fig. 6(a) is again the trend of the dissipated energy per cycle. Fig. 6(b) provides the evolution of the maximum and minimum values of stress for the three phases of the test. It seems that the healing process was able to work because it was introduced before significant compression stress were experienced by the specimen.

Such procedure of interrupting the test after a fraction of the specimen lifetime was repeated for test 6 in order to check that the previous result also holds for a temperature different from 30 °C.

Thus, with reference to test 6 in Table 1, the test is repeated (test 7) by interrupting it after 800

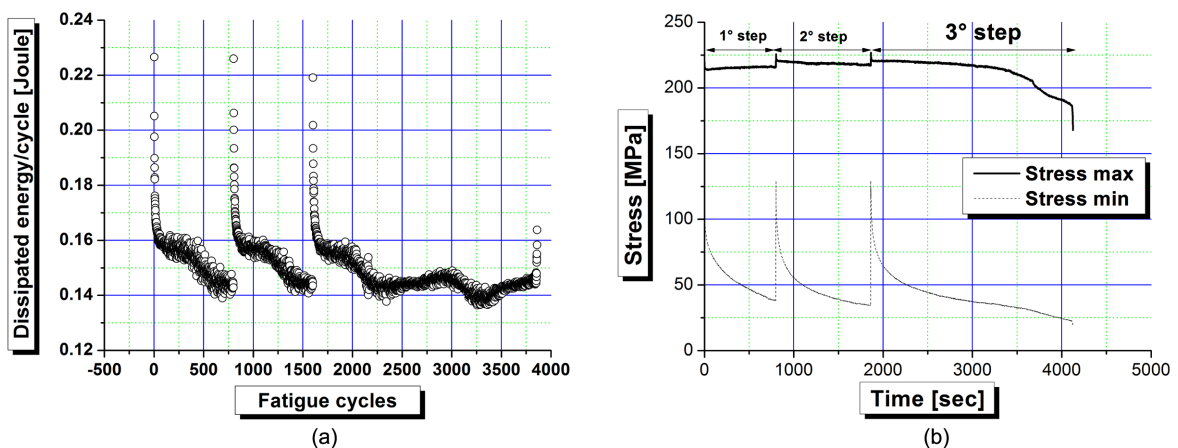


Fig. 7 Fatigue test between 1.2% and 4.3% of strain at 50 °C: first part of the test up to 800 cycles; second part of the test with further 800 cycles; third part of the test with further 2261 cycles. (a) energy dissipated per cycle and (b) maximum and minimum stresses as the cycles proceed

cycles. The thermal treatment which completes the initial preparation (1/2 hour at 280 °C) is repeated. The test re-starts and stops again after further 800 cycles and new thermal treatment. Eventually, third stage of the test up to final rupture. Fig. 7(a) is again the trend of the dissipated energy per cycle: here the relation shows some oscillations which could also be due to the modest number (16) of sampling point per cycle adopted. In any case this behavior requires a further investigation. Fig. 7(b) provides the evolution of maximum and minimum values of stress for the three phases of the test. In this case no compression stress was introduced; nevertheless, after a lower bound of the stress was reached in the third step, limit which was never reached in the two steps before, the path to failure accelerates.

## 5. A further set of fatigue tests

Fatigue tests were also conducted in span control during the loading and load control during the unloading. This allows one to complete the stress cycle (up to a vale and then down to zero), but the residual strain at the end of the cycle is the parameter to record.

In a different paper (Casciati and Marzi 2010), the test at  $\Theta = 30$  °C was presented with a preliminary mechanical treatment (see the note at the bottom of Table 1) and then cycles up to 3.2% of strain. The corresponding number of cycles was 2120. The preliminary thermal treatment consisted of 5 minutes at 850 °C, out at ambient temperature (water quenched), and finally 1 week at 100 °C.

It is worth being reported that when the specimen which underwent the shorter treatment was tested introducing and intermediate heating, the recover was successful. Fig. 8 provides the evolution of the energy dissipated along each cycle, the evolution of maximum and minimum stress as well as that of maximum and minimum strain. Fig. 9 provides the same graphs for the specimen with the longer thermal treatment (1 weeks) and make evident that the recover attempt in this case failed.

Thus one would conclude that there is a gate after which the damage phenomenon is no longer reversible (by heating), but this gate cannot be identified in terms of number of cycles. Fig. 9 would suggest to monitor the residual displacement (strain) after the unloading: once it reaches a threshold, the collapse becomes unavoidable.

Fig. 10 reports a similar successful test carried out at the temperature of 50 °C.

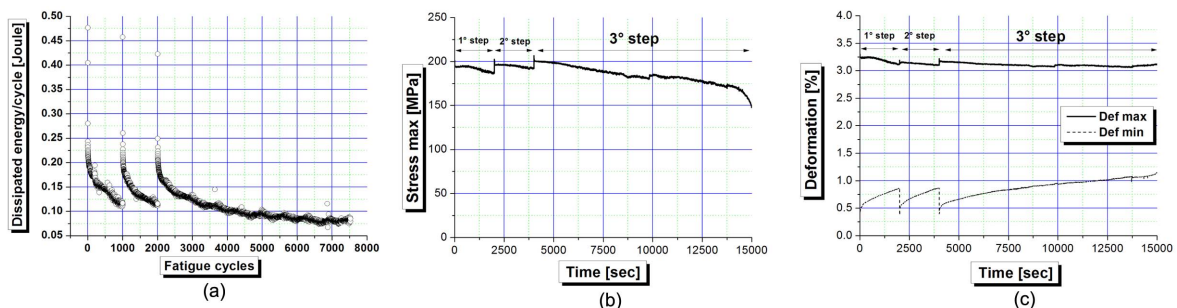


Fig. 8 Fatigue test with no preliminary mechanical treatment and then cycles up to 3.2% of strain and down to zero load,  $\Theta = 30$  °C

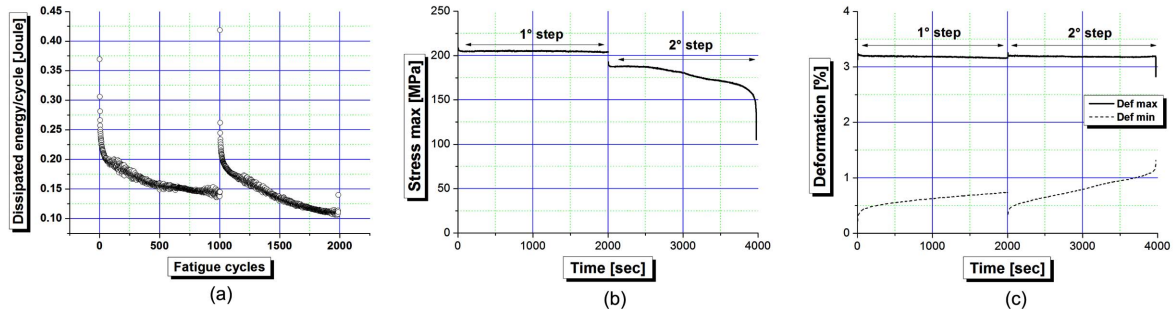


Fig. 9 Fatigue test as in Fig. 8, but on a specimen with initial thermal treatment of 1 week

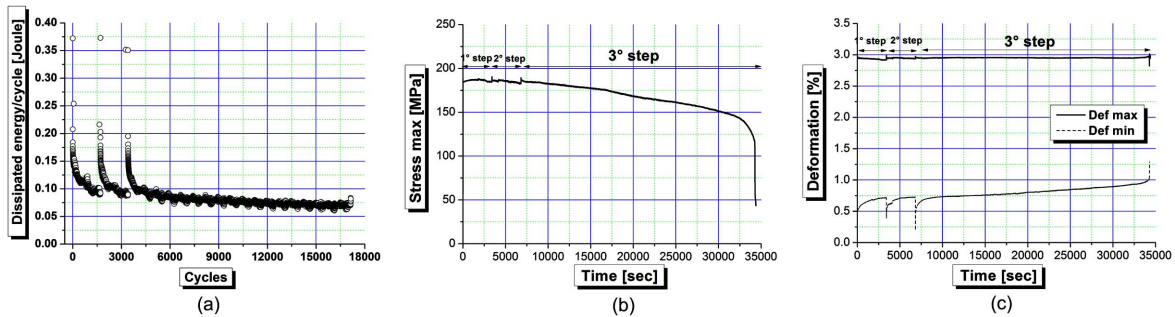


Fig. 10 Fatigue test with treatment and then cycles up to 3.0% of strain and down to zero load,  $\theta = 50\text{ }^{\circ}\text{C}$

## 6. Material recover and embedded informatics

The tests reported in sections 4 and 5 cover the fatigue performance of shape memory alloy bars in two possible scenarios of application:

- 1) partial loading/unloading around a pre-tensioned initial state (Casciati and Hamdaoui 2008); tests in span control to better follow the significant deformation variations associated with small stress modifications.
- 2) full loading/unloading from a zero load state initial state (Casciati *et al.* 2008). Here the tests were run in span control (for a better accuracy at high gradient of deformation) during the loading followed by a load control stage during the unloading to avoid compressions.

In both cases it was proved that an interruption of the test with a suitable thermal treatment can cancel the material memory restoring the initial durability. Two aspects require a further discussion:

- a. how the healing process can be automated?;
- b. which is the decisional parameter activating the thermal treatment?

In order to achieve self-healing features, one simply introduces embedded informatics, able to count the excitation peak (or to assess the current value of the decisional parameter) and to activate automatically, at a fixed threshold, a suitable heating of the alloy. The fatigue lifetime of a structural component, which underwent loading-unloading cycles, is made equal, after each thermal treatment, to the lifetime expected for its full replacement. The implementation does not require a quite complex technology. The sensors will report to a near-by electronic board (or to one linked by any wireless scheme (Casciati *et al.* 2009) mounting a microcontroller able to

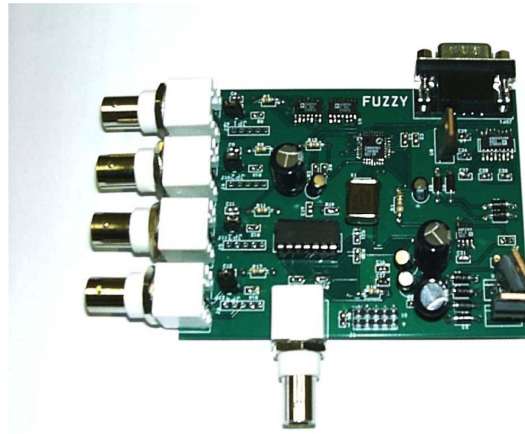


Fig. 11 Microcontroller showing 4 input channels and 1 output from which the annealing is started

perform the required computations and checks (Fig. 11). When the threshold is reached, by the selected decisional parameter, the thermal equipment is activated and the original lifetime recovered.

The basic issue is now which will be the decisional parameter? Indeed, the number of cycles, which in fatigue studies generally plays the key role, does not seem not to be the best candidate in this case, as the different result achieved in Figs. 8 and 9 shows. A test under equal conditions, except for the initial thermal treatment, recovered successfully in Fig. 8 and failed to recover in Fig. 9, despite that both the tests were interrupted for the thermal treatment after the same number of cycles.

Several additional experiments confirmed that the recover strongly depends on the time instant at which the test is interrupted and this instant cannot be simply linked to the lifetime of an uninterrupted reference fatigue test.

Such remarks led the authors to consider several different quantities as decisional parameter:

- 1) for tests in span control, where maximum and minimum strains are assigned, the minimum and maximum stresses in each cycles were considered. It is seen, in Figs. 6(b) and 7(b), that the maximum stress decreases significantly only when the specimen failure is approached. Thus, the minimum stress  $\sigma_{\min}$  seems to be a more reliable index. It decreases with positive second derivative in time until either a threshold is reached or a slope discontinuity is outlined. The sensor required in this case is just a load cell monitoring the bar load.
- 2) for tests in span control during loading and load control during unloading, the quantities which define the test are the maximum strain and the minimum null stress. Thus the minimum strains and the maximum stress, in each cycle, are the candidates to be considered as decisional parameter. It is seen in Figs. 8(b) and 8(c), 9(b) and 9(c) and 10(b) and 10(c), that again the maximum stress decreases significantly only when the specimen failure is approached. But the minimum strain  $\varepsilon_{\min}$  seems to be a reliable index: when a value of 0.7-0.8% is reached the fatigue test should be interrupted and the thermal treatment done in order to reach the full recover. This was not the case of Fig. 9(c) and the failure was reached during the test. Two sensors are required in this case is: a load cell monitoring the bar load and an LVDT (linear variable differential transducer) or a more sophisticated sensor for measuring the bar

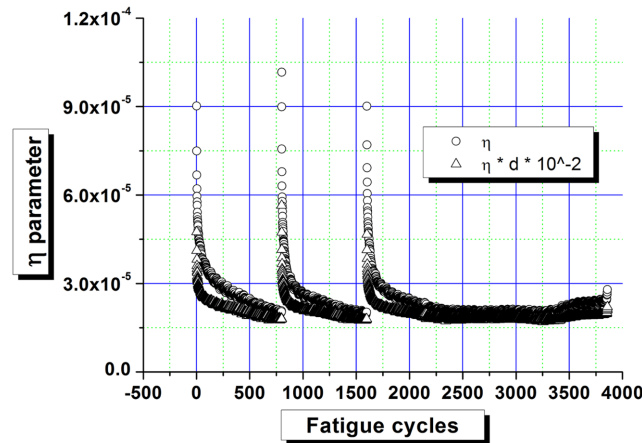


Fig. 12 Fatigue test between 1.2% and 4.3% of strain at 50 °C: first part of the test up to 800 cycles; second part of the test with further 800 cycles; third part of the test with further 2261 cycles. Time histories of the parameter  $\eta$  and of the elliptic cycle radius  $\eta d$

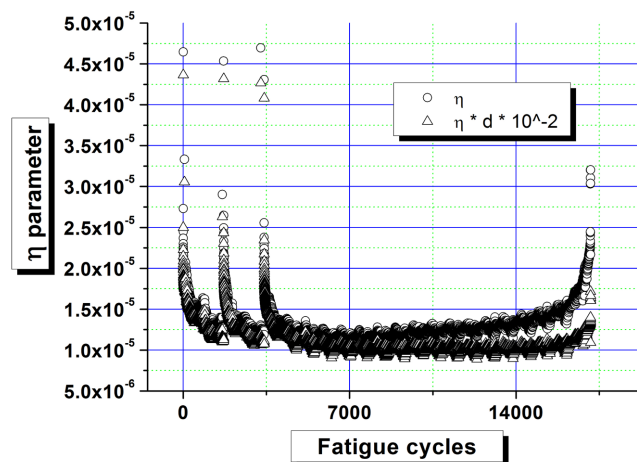


Fig. 13 Fatigue test with treatment and then cycles up to 3.0% of strain and down to zero load,  $\theta = 50$  °C

elongation.

- 3) with the availability of two sensors, covering both statics and kinematics, one can compute the energy per cycle, as shown in Figs. 6(a), 7(a), 8(a), 9(a) and 10(a). It is evident that the deterioration process can be stopped until the energy is above a threshold, but unfortunately, the value of the threshold is difficult to be established before running the test. For this reason, the quantity  $\eta d$  (Eq. (4)) was computed. Its time histories in the cases of Figs. 7 (span control) and 10 (span and load control) are shown in Figs. 12 and 13 respectively. It is seen that the time derivative tends to zero and hence the tests have to be interrupted when the derivative of  $\eta d$  is still negative.
- 4) Figs. 12 and 13 also contain the plots in time of the dimensionless parameter  $\eta$ . The plots show that the time derivative of the variable increases and crosses the null value. This null value can be conveniently selected as the threshold, i.e., the time for interrupting the test. This

make  $\eta$  a very attractive decisional parameter.

The final problem which is worth mentioning is that the actual loading-unloading cycles, which the alloy component will undergo during its real life, are not characterized by constant strain ranges, so that a decisional parameter independent of the cycles amplitude should be pursued. Two cases must be distinguished: i) the excitation intensity spans from a given value to a variable maximum; ii) the excitations intensity spans around a reference value between two variable values.

In the first case the decisional parameters in 2) and 4) still work and hence they can be used also for loading-unloading cycles of different amplitude. By contrast, in the second case, only the decisional parameter in 4), i.e., the dimensionless quantity  $\eta$ , could result unaffected by the variability of the loading-unloading cycles. Up to now, no tests with cycles of variables amplitude were accomplished and the validity of this decisional parameter has still to be checked in the laboratory.

## 7. Conclusions

A recent study (Casciati *et al.* 2008) (also co-authored by the first author) emphasized the inadequacy of structural components made of a special Cu-based shape memory alloy to undergo a very high number of loading-unloading cycles. Nevertheless, simple thermal treatments are able to cancel the memory of the material on the previously undergone damage. This thermal healing is experimentally shown in this contribution by fatigue tests on pre-tensioned bars where the load oscillations span across the so-called plateau of the alloy constitutive law.

The investigated problem is then how to realize a cycle-counter, or better to identify the threshold for a suitable decisional parameter, to be coupled with a simple software alerting for the deterioration and asking for the thermal treatment able to produce the full recover of the material.

## Acknowledgments

A grant from the Athenaeum Research Funds (FAR) is acknowledged. The authors are grateful to the journal referees for their constructive remarks.

## References

- AFOSR/ARO/NSF/ONR/ESF (2006), *Proceedings of the Jointly Sponsored Workshop on Smart Systems for Mitigation of Exogenous Threats Using Autonomic Response*, Juan les Pins, France.
- Auricchio, F., Faravelli, L., Magonette, G. and Torra, V. (Eds.) (2001), *Shape Memory Alloys: Advances in Modelling and Applications*, CIMNE, Barcelona, Spain.
- Brailovski, V., Terriault, P. and Prokoshkin, S. (2002), "Influence of the post-deformation annealing heat treatment on the low-cycle fatigue of NiTi shape memory alloys", *J. Mater. Eng. Perform.*, **11**(6), 614-621.
- Casciati, F., Casciati, S. and Faravelli, L. (2007), "Fatigue characterization of a cu-based shape memory alloy", *Proc. Estonian Acad. Sci. Phys. Math.*, **56**(2), 207-217.
- Casciati, F. and Faravelli, L. (2009), "A passive control device with SMA components: from the prototype to the model", *J. Struct. Control Health Monit.*, **16**(7-8), 751-765.
- Casciati, F., Faravelli, L., Isalgue, A., Martorell, F., Soul, H. and Torra, V. (2008), "SMA fatigue in civil engineering applications", *Proceedings of the CIMTEC '08*, Acireale, Sicily, Italy, June.

- Casciati, F. and Van der Eijk, C. (2008), "Variability in mechanical properties and microstructure characterization of CuAlNi shape memory alloys for vibration mitigation", *Smart Struct. Syst.*, **4**(2), 103-121.
- Casciati, S. (2007) "Thermal treatment optimization for Cu-based shape memory alloys", *Proceedings of the First International Conference on Self Healing Materials*, Noordwijk aan Zee, The Netherlands, April.
- Casciati, S., Chen, Z. and Faravelli, L. (2009), "Design of a multi-channel real-time wireless connection system for analog cable replacement", *Proceedings of the 7th International Workshop on Structural Health Monitoring (IWSHM)*, **1**, 886-893.
- Casciati, S. and Faravelli, L. (2006), "Fatigue tests of a Cu-based shape memory alloy", *Proceedings of the 4th World Conference on Structural Control and Monitoring*, San Diego, CA, USA, July.
- Casciati, S. and Faravelli, L. (2008), "Structural components in shape memory alloy for localized energy dissipation", *Comput. Struct.*, **86**(3-5), 330-339.
- Casciati, S. and Hamdaoui, K. (2008), "Experimental and numerical studies toward the implementation of shape memory alloy ties in masonry structures", *Smart Struct. Syst.*, **4**(2), 153-169.
- Casciati, S. and Marzi, A. (2010), "Experimental studies on the fatigue life of shape memory alloy bars", *Smart Struct. Syst.*, **6**(1), 73-85.
- Casciati, S. and Rossi, R. (2006), "Embedding SHM algorithms into a microcontroller for real-time and fully automated civil applications", *Proceedings of the Third European Workshop on Structural Health Monitoring*, (Ed. Guemes, A.), Granada, Spain, July.
- Chrysostomou, C.Z., Stassis, A., Demetriou, T. and Hamdaoui, K. (2008), "Application of shape memory alloy prestressing devices on an ancient aqueduct", *Smart Struct. Syst.*, **4**(2), 261-278.
- Ding, H.S., Lee, J.M., Lee, B.R., Kang, S.B. and Nam, T.H. (2007), "Effects of subsequent heat treatment on the shape memory behaviors of a Ti/Ni sheet fabricated by bonding and cold rolling of Ti/Ni multilayers", *Mat. Sci. Eng. A-Struct.*, **444**(1-2), 265-270.
- Dolce, M. and Cardone, D. (2005), "Fatigue resistance of SMA-martensite bars subjected to flexural bending", *Int. J. Mech. Sci.*, **47**(11), 1693-1717.
- Faravelli, L. (2008), "Embedded informatics toward a metallic self-healing material", *Proceedings of the 4th European Conference on Structural Control*, St. Petersburg, Russia, September.
- Faravelli, L., Rossi, R. and Torelli, G. (2003), "Numerical testing of a programmable microcontroller with fuzzy and adaptive features", *Simul. Model. Pract. Th.*, **11**(5-6), 421-431.
- Nayan, N., Roy, D., Buravalla, V. and Ramamurty, U. (2008), "Unnotched fatigue behavior of an austenitic Ni-Ti shape memory alloy", *Mat. Sci. Eng. A-Struct.*, **497**(1-2), 333-340.
- Shimamoto, A., Zhao, H.Y. and Abé, H. (2004), "Fatigue crack propagation and local crack-tip strain behaviour in TiNi shape memory fiber reinforced composite", *Int. J. Fatigue*, **26**(5), 533-542.
- Tabanlı, R.M., Simha, N.K. and Berg, B.T. (1999), "Mean stress effects on fatigue of NiTi", *Mat. Sci. Eng. A-Struct.*, **273-275**, 644-648.
- Terriault, P., Torra, V., Fischer, C., Brailovski, V. and Isalgue, A. (2007), "Superelastic shape memory alloy damper equipped with a passive adaptive pre-straining mechanism", *Proceedings of the 9th Canadian Conference on Earthquake Engineering*, Ottawa, ON, Canada, June.
- Torra, V., Isalgue, A., Auguet, C., Lovey, F.C., Pelegrina, J.L. and Terriault, P. (2007), "Pre-stressed NiTi: effects of the thermodynamic forces and time", *Proceedings of The International Conference on Shape Memory and Superelastic Technologies (SMST)*, Tsukuba, Japan, December.
- Van der Zwaag, S. (Ed.) (2007), *Self-healing Materials*, Springer Verlag, Dordrecht, The Netherlands.
- Van Humbeeck, J. (1991), "Cycling effects, fatigue and degradation of shape memory alloys", *J. de Physique IV*, **1**(C4), 189-197.